Fabrication of Free-Standing Hybrid Nanosheets Organized with Polymer Langmuir−Blodgett Films and Gold Nanoparticles

Hiroshi Endo, Yuko Kado, Masaya Mitsuishi,* and Tokuji Miyashita*

Institute of Multidisciplinary Research for Advanced Materials (IMRAM), Tohoku University, 2-1-1 Katahira, Aoba-ku, Sendai 980-8577, Japan

Received November 11, 2005
Revised Manuscript Received March 23, 2006

Introduction

A robustly and beautiful patterned textile is made from a two-dimensional surface through the crossing of the warp and weft, creating various textures such as stripes, plaids, wood, leaves and brick. etc. Moreover, yarn is a fiber assembly consisting of many polymers. These assemblies, which consist of sophisticatedly organized components, can be imitated at the nanometer scale for development of novel microdevices or nanodevices. Such robustly strengthened textiles with the thickness in nanoscale can function as free-standing ultrathin films that can be useful as next-generation sensing membranes for various fields.[1−3] In fact, various approaches to fabricate free-standing films have been reported. Hashizume and Kunitake prepared a free-standing film of titania by spin-coating.[4] Mallwitz and Goedel prepared a physically cross-linked elastomeric free-standing film using the Langmuir−Blodgett (LB) method.[5] Moreover, Mamedov and Kotov prepared a free-standing film containing magnetic nanoparticles[6a] or carbon nanotubes[6b] by electrostatic layer-by-layer assembly. They claim the importance of hybridization between these inorganic materials and polymer to enhance the film strength.[6c] Furthermore, it is necessary to improve not only mechanical strength in three-dimensions, but also smoothness in a two-dimensional surface for fabrication of smoothly and robustly nanotextured free-standing films. Such free-standing films with smooth surfaces in a large area will provide a plane, as a canvas, upon which other functional molecules can be applied and organized.

Previously, we reported that *N*-alkylacrylamide homopolymers and its copolymers with various functional groups form a highly oriented polymer monolayer on a water surface through a two-dimensional hydrogen-bonding network between amide groups. The self-assembled hydrogen-bonding network provides densely packed and stable polymer monolayer formation and multilayer deposition using the LB method.[7,8] The LB technique enables fine control at nanoscale thickness and homogeneity of monolayers along with ease of multilayer deposition,[9,10] compared to other techniques such as spin-cast, vapor deposition, or self-assembled monolayers. By using polymer LB films with excellent properties, we developed ultrathin functional devices for biosensors,[11] pH sensors,[12] photodevices and electrodevices,[13−17] and optical logic gates.[18,19] From insights gained through their construction, we have called these functional ultrathin polymer LB films "polymer nanosheets". Moreover, we have controlled gold nanoparticle adsorption onto polymer nanosheets.[20] Recently, we robustly immobilized multilayered polymer nanosheets onto the substrate by using photopolymerization of methacryloyl group incorporated into the polymer nanosheets by deep UV irradiation.[21] The immobilized nanosheets have great mechanical and chemical stability because of a 3-D photocrosslinking network in polymer nanosheets. Moreover, the fabrication of unique 3-D nanostructures proved the smoothness of their film, resulting in a beautiful interference color appearance corresponding to each film thickness. Accordingly, it will be expected that using this photoreactive nanosheet will produce a smooth, robust, and highly organized free-standing nanosheet.

This paper presents a description of the fabrication of free-standing ultrathin polymer films with reactive polymer nanosheets. The photocrosslinkable polymer nanosheets were hybridized with gold nanoparticles, thereby enabling visualization of the ultrathin film more easily because of its strong extinction coefficient. The materials were strengthened mechanically through a photocrosslinking reaction. The ultrathin free-standing films thus obtained are flexible and stable, with nanometer thickness.

Experimental Section

Materials. *N*-Dodecylacrylamide (DDA) was synthesized according to a previous report.[22] DDA copolymers containing terminal amino groups (2,2′-(ethylenedioxy)bis(ethylamine) (DADOO)) in side chains (pDDA−DADOO) or a methacryloyl group in the side chains (pDDA−M) were also synthesized according to previous reports.[21,23] Figure 1 shows chemical structures of the polymer nanosheet. Monodispersed gold nanoparticles were prepared through reduction of $HAuCl_4$ with sodium citrate in water at 100 °C.[24] The average gold nanoparticle diameter was estimated as approximately 30 nm by using transmission electron microscopy (TEM).

Monolayer Formation. All polymers were spread onto the water surface from a chloroform solution. Surface pressure (π)−area (A) isotherms and LB film deposition were carried out using an automatically controlled Langmuir trough (FSD-220 & 21; U.S.I. System) The pDDA, pDDA−DADOO, and pDDA−M monolayers can be transferred respectively onto solid substrates as Y-type LB films at a surface pressure of 30 mN/m at 15 °C, 35 mN/m at 15 °C, and 35 mN/m at 20 °C.

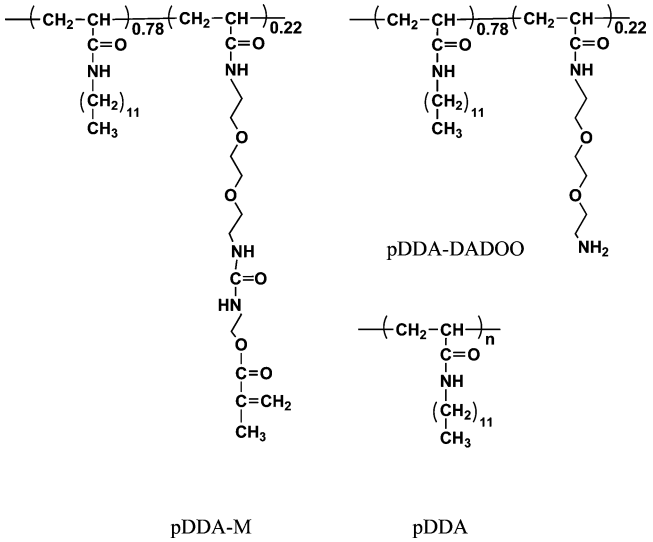

Figure 1. Chemical structures of pDDA−DADOO, pDDA−M, and pDDA.

* To whom correspondence should be addressed. E-mail: masaya@tagen.tohoku.ac.jp (M.M.); miya@tagen.tohoku.ac.jp (T.M.). Telephone: +81-22-217-5638. Fax: +81-22-217-5638.

10.1021/ma052410j CCC: $33.50
Published on Web 07/13/2006

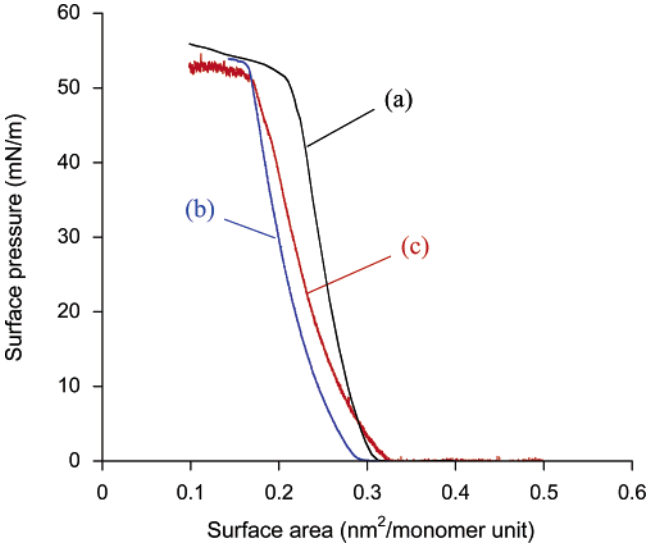

Figure 2. $\pi-A$ isotherms of (a) pDDA, (b) pDDA−DADOO, and (c) pDDA−M at 20 °C.

Measurements. Atomic force microscopy images were taken with the DFM mode (SPA400; Seiko Instruments Inc.). The XPS spectra were obtained using an X-ray photoelectron spectrometer (ESCA 5300; Perkin Elmer Inc.). The UV absorption measurements were carried out with a UV−vis spectrophotometer (U-3000; Hitachi Ltd.). All measurements were carried out at room temperature.

Results and Discussion

Ultrathin Film Formation. Figure 2 shows $\pi-A$ isotherms of copolymers at 20 °C. They give a steep rise in surface pressure and high collapse pressure, indicating that all polymers form densely packed monolayers at the water surface. Respective polymer monolayers were transferred on solid substrates with a good transfer ratio. In Figure 3 is shown schematic illustration of the preparation of free-standing hybrid ultrathin nanosheets. For construction of a free-standing hybrid nanosheet, the chloroform-soluble pDDA nanosheets with 10 layers were first deposited as a sacrificial soluble layer onto the hydrophobized substrate (quartz plate or silicon wafer). Subsequently, two-layer pDDA−DADOO nanosheets containing terminal amino groups were deposited onto the pDDA layers (Figure 3a). The substrate was immersed in gold nanoparticles (approximately 30 nm in an average diameter) aqueous solution overnight (Figure 3b). After adsorption of gold nanoparticles, the substrate was rinsed with pure water and then dried with nitrogen gas. Next, 14-layer pDDA−M nanosheets containing photocrosslinkable methacryloyl terminal groups were transferred onto the gold nanoparticles monolayer (Figure 3c). Then the film was photoirradiated using a deep UV lamp (UXM-501MA; USHIO Inc., 70 mW/cm^2) in air atmosphere for 10 min (Figure 3d). Previously, we observed the change in absorbance at 197 nm under deep UV irradiation, which is assigned to amide bonding in the pDDA−M nanosheet after immersion in chloroform.[21] Results revealed that the photopolymerization of methacryloyl groups, both internanosheets and intrananosheets, was completed within 10 min. Finally, the substrate was slowly dipped into a chloroform solution (Figure 3e) to dissolve the sacrificial pDDA layers. Finally, we were able to peel off an ultrathin pDDA−M/gold nanoparticle-composite nanosheet (over 50 mm^2) (Figure 3f**)**. A transmission electron microscope (TEM) grid (85 μm diameter) was used to hold the free-standing hybrid nanosheet (Figure 3g). Most of the circular holes of the TEM grid were covered with the free-standing hybrid nanosheet, which is brighter than other areas because of the light reflection from the free-standing film. Free-standing hybrid nanosheets on the TEM grid were stable for at least one month without corruption. Moreover, the free-standing hybrid nanosheet on a TEM grid with larger rectangular hole dimensions of 280 μm × 280 μm showed no important damage for several months. These results indicate that the free-standing

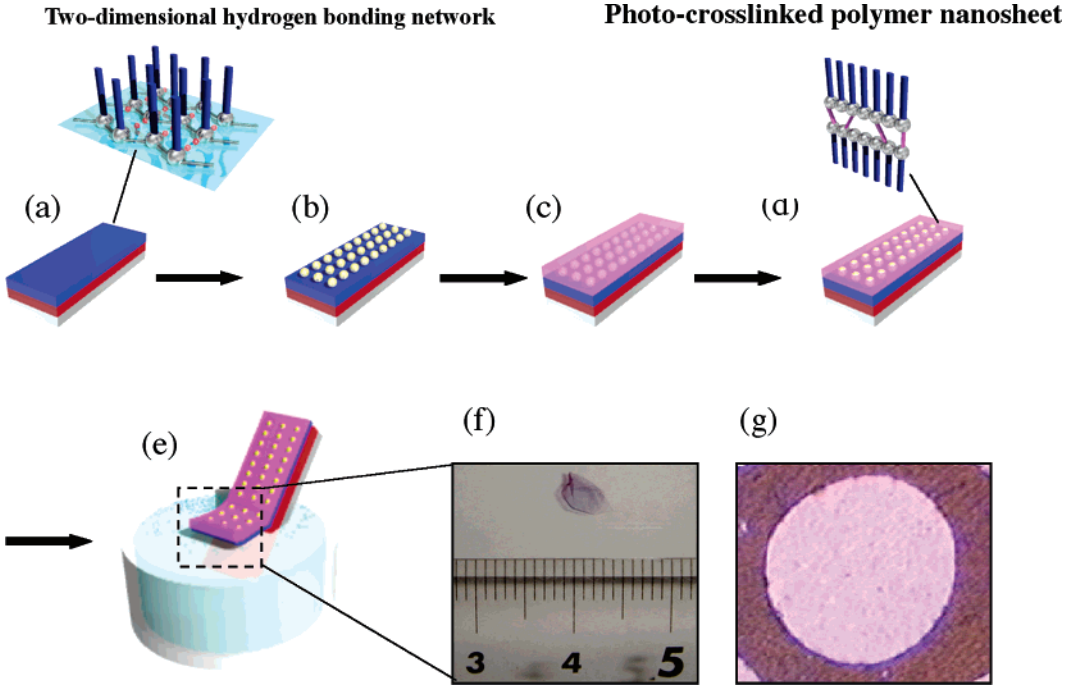

Figure 3. Schematic outline of the preparation of free-standing hybrid nanosheet: (a) the pDDA (10 layers) and pDDA−DADOO (2 layers) nanosheets were transferred onto a hydrophobized substrate, (b) immobilization of gold nanoparticles, (c) deposition of the pDDA−M nanosheets (14 layers), (d) UV irradiation, (e) immersion into chloroform solution, (f) photograph of free-standing hybrid nanosheet on a chloroform surface, and (g) optical micrograph of free-standing hybrid nanosheet on a copper TEM grid with 85 μm holes.

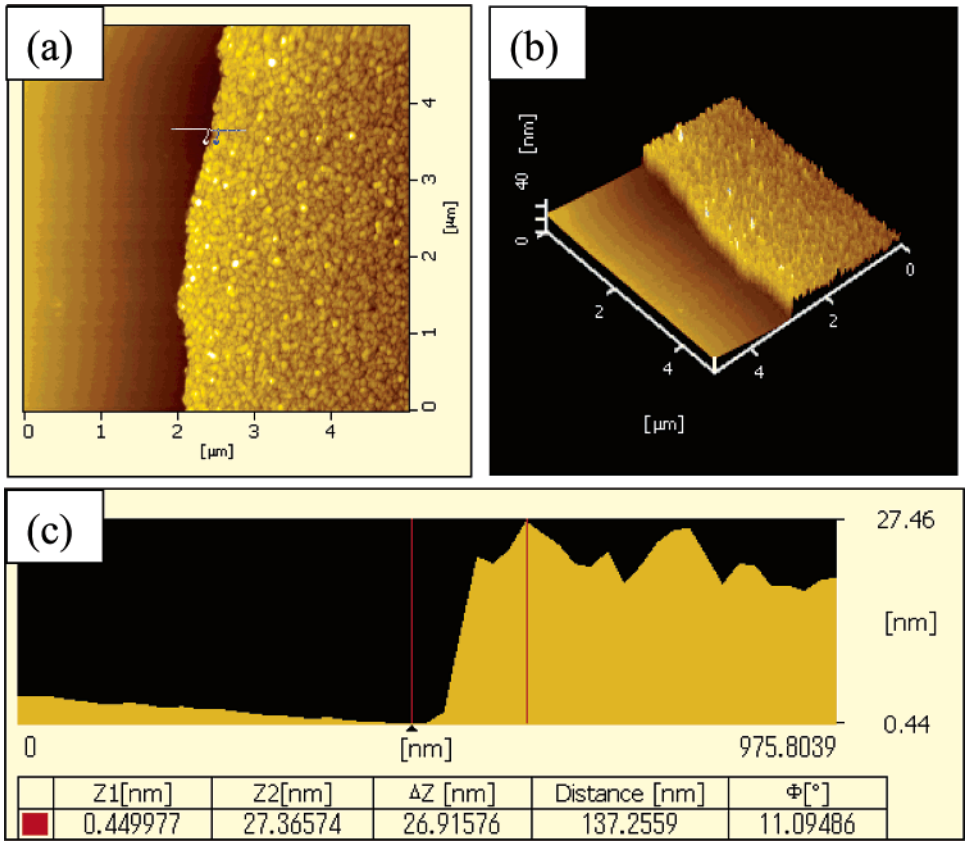

Figure 4. AFM image of the released nanosheet edge on a silicon wafer surface: (a) top view, (b) 3-D image, and (c) cross section of image (a).

ultrathin film is strengthened robustly by hybridization with gold nanoparticles on a nanoscale.

Surface Morphology of Free-Standing Film. Figure 4 shows atomic force microscopy (AFM) images of the released nanosheet edge on a silicon wafer surface. A free-standing photocrosslinked polymer nanosheet was obtained; gold nanoparticles were embedded in polymer nanosheets over a large area. Root-mean-square (rms) roughness of the film surface showed a marvelously smooth surface (under 5 nm) compared with the free-standing film surface containing gold nanoparticles (12.7 nm diameter) produced by layer-by-layer assembly[25] even though the gold nanoparticle's diameter is larger. This result suggests that densely packed polymer nanosheets provide a smooth surface at the nanometer level. The film thickness was estimated as approximately 30 nm, corresponding to the gold nanoparticle diameter.

Two different systems were examined using AFM observation to confirm the difference of surface morphology before and after UV irradiation (Figure 5). Parts a and b of Figure 5 show pDDA−M nanosheets with four layers deposited onto a gold nanoparticle monolayer. After UV irradiation, an increase in rms from 3.3 to 5.2 nm was observed along with morphological changes of the film, which might be attributable to changes in packing of pDDA−M nanosheets before and after the UV irradiation. The free-standing nanosheet, however, was not detachable from the substrate after immersion into a chloroform solution in this condition. Mechanical strength of pDDA−M nanosheets with four layers might be too little to maintain it in a chloroform solution. In the case of pDDA−M nanosheets with 14 layers deposited onto a gold nanoparticle monolayer (Figure 5c and d), it was observed that gold nanoparticle monolayers became smoother after a photocrosslinking reaction of pDDA−M nanosheets. Furthermore, C 1s, N 1s, and O 1s peaks at 284.6, 399.6, and 532.5 eV were observed from the released film surface on the silicon wafer by X-ray photoelectron spectroscopy (XPS) measurements (Figure 6). These peaks are attributable to the polymer chains of pDDA−M nanosheets. Therefore, the detachment experiment proved that the pDDA−M nanosheets with 14 layers (ca. 28 nm) were necessary to construct free-standing nanosheets. The film thickness corresponds to the gold nanoparticles' diameter. Surface coverage of the gold nanoparticles is approximately 42%, as calculated from the scanning electron microscopy (SEM) image. Some pDDA−M nanosheets were removed from the surface under deep UV irradiation in the air atmosphere and immersion in a chloroform solution. The remaining pDDA−M nanosheets undergo the photocrosslinking reaction and structural relaxation through thermal relaxation. These findings indicate that the pDDA−M nanosheets act not only as a coated film, but also as a binder to hold gold nanoparticles firmly. It was difficult to peel off a free-standing nanosheet from the substrate precoated with less than 10-layer pDDA nanosheets as a sacrificial layer. Considering that the monolayer thickness of pDDA is 1.72 nm, at least 17 nm thickness is necessary as a sacrificial layer to peel off a free-standing nanosheet safely.

UV−Vis Absorption Spectra of Free-Standing Film. Figure 7 shows UV−vis absorption spectra of a free-standing nanosheet during respective preparation processes. Two broad peaks were visible in the region of 500−700 nm after immersion into the gold nanoparticle solution.[26] These peaks indicate individual and collective surface plasmon resonance by gold nanoparticles adsorbed onto pDDA−DADOO nanosheet. After UV irradiation, absorbance of the broad peak around 670 nm was increased slightly. That increase implies that no substantial fusion among gold nanoparticles was observed during UV irradiation. In fact, SEM images of the gold nanoparticles show no changes in the

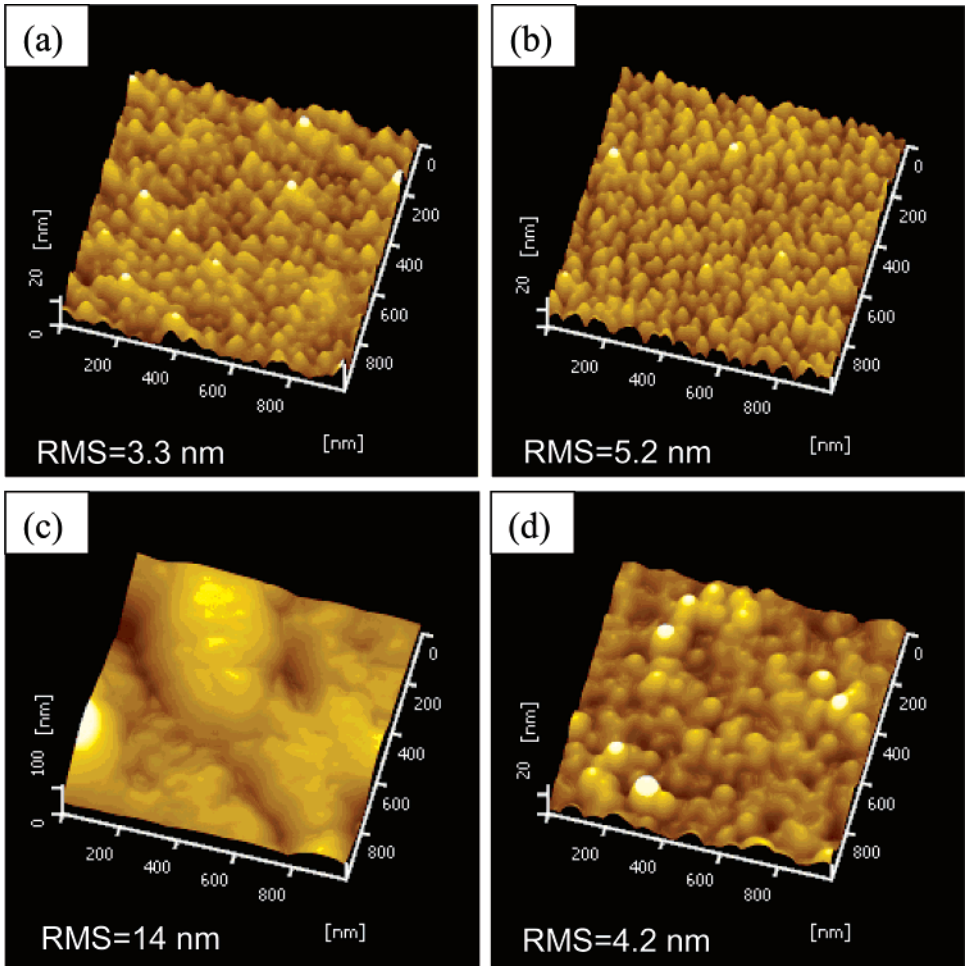

Figure 5. AFM image of pDDA−M nanosheets with a gold nanoparticle layer: (pDDA−M four layers) (a) before and (b) after irradiation; (pDDA−M 14 layers) (c) before and (d) after irradiation. Inset: root-mean-square (RMS) roughness value.

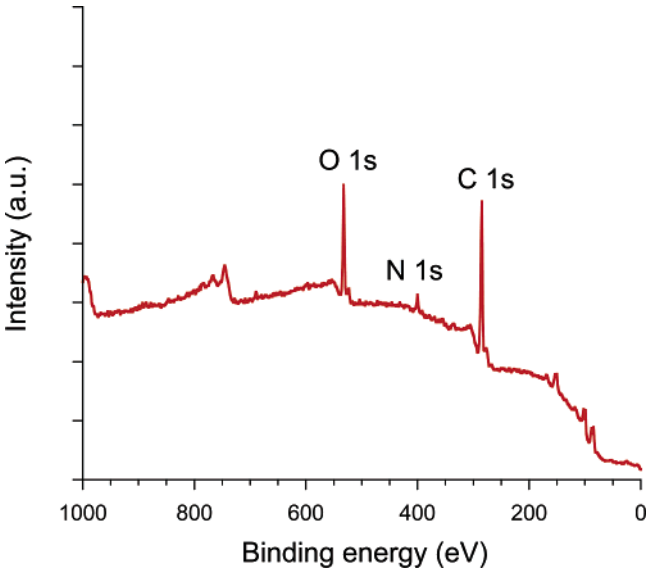

Figure 6. XPS wide scan spectra of free-standing film surface.

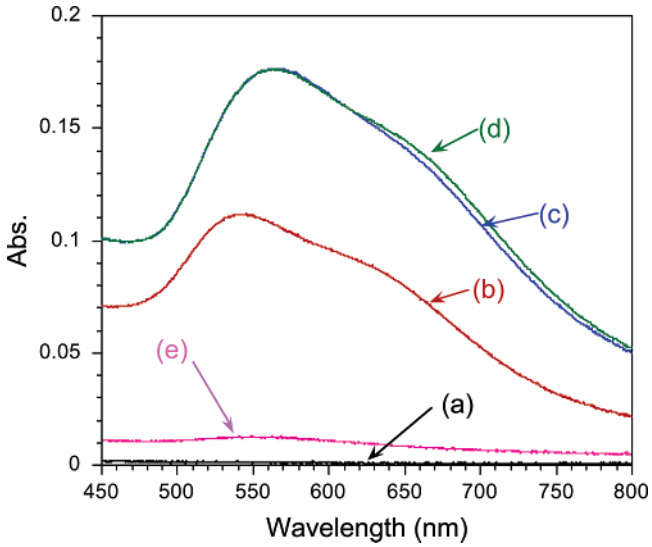

Figure 7. UV−Vis absorption spectra for each stage in the preparation procedure of a free-standing nanosheet: (a) the pDDA (10 layers) and pDDA−DADOO (two layers) nanosheets were transferred onto a quartz plate, (b) immobilization of gold nanoparticles, (c) deposition of the pDDA−M nanosheets (14 layers), (d) UV irradiation, and (e) immersion into a chloroform solution.

gold nanoparticle array before and after UV irradiation (Figure 8). After immersion into chloroform solution, the absorbance disappeared dramatically. This result also indicates that the free-standing nanosheet was peeled off from the substrate.

In conclusion, we demonstrated the fabrication of a giant and well-organized free-standing hybrid nanosheet consisting of gold nanoparticles and photocrosslinkable polymer LB films. The minimum film thickness was estimated as 30 nm. Moreover, the hybrid nanosheet shows a smooth surface with 5 nm roughness. Gold nanoparticles enable visualization of the nanosheet and strengthen the film mechanically (filler effect).

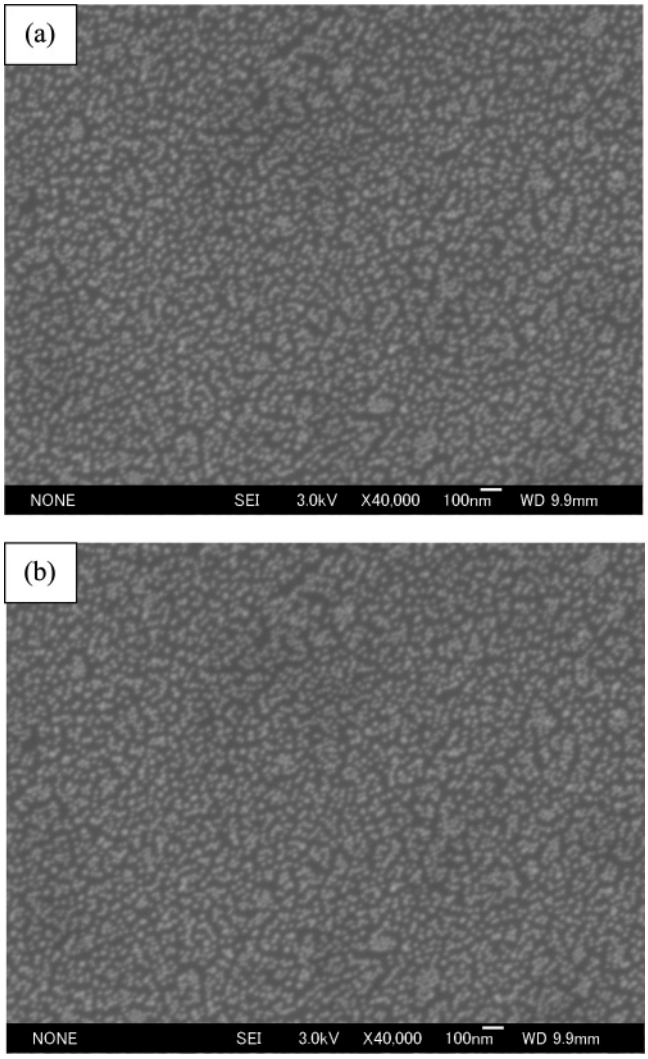

Figure 8. SEM images of gold nanoparticle monolayer before (a) and after (b) UV irradiation.

We anticipate fabrication of hybrid free-standing ultrathin films, but we also look forward to the future addition of various functions that can be achieved through control of particle size and utilization of other particles such as metallic, magnetic, and semiconducting nanoparticles.

Acknowledgment. We thank Mr. Masuo Ito, IMRAM, Tohoku University, for XPS observation and the Hybrid Nano-Materials Research Center (HyNaM Center) for the use of AFM and E-SEM. This work was supported by a grant-in-aid for scientific research (S) (no. 17105006) from the Japanese Ministry of Education, Culture, Sports, Science, and Technology, and the Mitsubishi Foundation. This work was carried out as one project in the "Materials Science & Technology Research Center for Industrial Creation (MSTeC)".

References and Notes

(1) Jiang, C.; Markutsya, S.; Pikus, Y.; Tsukruk, V. V. *Nat. Mater*. **2004**, *3*, 721.
(2) Feng, H.; Tianhong, C.; Yuri M. L. *Nano Lett.* **2004**, *4*, 823.
(3) Phadtare, S.; Vinod, V. P.; Wadgaonkar, P. P.; Rao, M.; Sastry, M. *Langmuir* **2004**, *20*, 3717.
(4) Hashizume, M.; Kunitake, T. *Langmuir* **2003**, *19*, 10172.
(5) Mallwitz, F.; Goedel, W. A. *Angew. Chem., Int. Ed.* **2001**, *40*, 2645.
(6) (a) Mamedov, A. A.; Kotov, N. A. *Langmuir* **2000**, *16*, 5530. (b) Mamedov, A. A.; Kotov, N. A.; Prato, M.; Guldi, D. M.; Wicksted, J. P.; Hirsch, A. *Nat. Mater*. **2002**, *1*, 190. (c) Shim, B. S.; Kotov, N. A. *Langmuir* **2005**, *21*, 9381.
(7) Miyashita, T. *Prog. Polym. Sci*. **1993**, *18*, 263.
(8) Taniguchi, T.; Yokoyama, Y.; Miyashita, T. *Macromolecules* **1997**, *30*, 3646.
(9) Kuhn, H.; Möbius, D.; Bücher, H. *Physical Methods of Chemistry, Part IIIB*; Wiley-Interscience: New York, 1972; Chapter VII.
(10) Gaines, G. L., Jr. In *Insoluble Monolayers at Liquid-Gas Interfaces*; Wiley-Interscience: New York, 1966.
(11) Ide, M.; Mitamura, A.; Miyashita, T. *Bull. Chem. Soc. Jpn.* **2001**, *74*, 1355.
(12) Kado, Y.; Aoki, A.; Miyashita, T. *Int. J. Nanosci.* **2002**, *5*−*6*, 637.
(13) Amao, Y.; Asai, K.; Miyashita, T.; Okumura, I. *Polym. J.* **1999**, *31*, 1267.
(14) Amao, Y.; Asai, K.; Miyashita, T.; Okumura, I. *Polym. Adv. Technol.* **2000**, *11*, 705.
(15) Aoki, A.; Miyashita, T. *Macromolecules* **1996**, *29*, 4662.
(16) Aoki, A.; Miyashita, T. *Electrochemistry* **2001**, *69*, 929.
(17) Fukuda, N.; Mitsuishi, M.; Miyashita, T. *J. Phys. Chem. B* **2002**, *106*, 7048.
(18) Matsui, J.; Mitsuishi, M.; Aoki, A.; Miyashita, T. *Angew. Chem., Int. Ed.* **2003**, *42*, 2272.
(19) Matsui, J.; Mitsuishi, M.; Aoki, A.; Miyashita, T. *J. Am. Chem. Soc.* **2004**, *126*, 3708.
(20) Tanaka, H.; Mitsuishi, M.; Miyashita, T. *Langmuir* **2003**, *19*, 3103.
(21) Kado, Y.; Mitsuishi, M.; Miyashita, T. *Adv. Mater.* **2005**, *17*, 1857.
(22) Arisumi, K.; Feng, F.; Miyashita, T.; Ninomiya, H. *Langmuir* **1998**, *14*, 5555.
(23) Kado, Y.; Aoki, A.; Miyashita, T. *J. Mater. Sci.* **2002**, *37*, 4839.
(24) Kawaguchi, T.; Tagawa, K.; Senda, F.; Matsunaga, T.; Kitano, H. *J. Colloid Interface Sci.* **1999**, *210*, 290.
(25) Jiang, C.; Markutsya, S.; Tsukruk, V. V. *Adv. Mater.* **2004**, *16*, 157.
(26) Jiang, C.; Markutsya, S.; Tsukruk, V. V. *Langmuir* **2004**, *20*, 882.

MA052410J